Title	Time-resolved photoluminescence measurements for determining voltage-dependent charge-separation efficiencies of subcells in triple-junction solar cells
Author(s)	Tex, David M.; Ihara, Toshiyuki; Akiyama, Hidefumi; Imaizumi, Mitsuru; Kanemitsu, Yoshihiko
Citation	Applied Physics Letters (2015), 106(1)
Issue Date	2015-01-05
URL	http://hdl.handle.net/2433/192939
Right	Copyright 2015 American Institute of Physics. This article may be downloaded for personal use only. Any other use requires prior permission of the author and the American Institute of Physics.
Type	Journal Article
Textversion	publisher

AIP | Applied Physics Letters

Time-resolved photoluminescence measurements for determining voltage-dependent charge-separation efficiencies of subcells in triple-junction solar cells

David M. Tex, Toshiyuki Ihara, Hidefumi Akiyama, Mitsuru Imaizumi, and Yoshihiko Kanemitsu

Citation: Applied Physics Letters **106**, 013905 (2015); doi: 10.1063/1.4905474
View online: http://dx.doi.org/10.1063/1.4905474
View Table of Contents: http://scitation.aip.org/content/aip/journal/apl/106/1?ver=pdfcov
Published by the AIP Publishing

Time-resolved photoluminescence measurements for determining voltage-dependent charge-separation efficiencies of subcells in triple-junction solar cells

David M. Tex,[1] Toshiyuki Ihara,[1] Hidefumi Akiyama,[2] Mitsuru Imaizumi,[3] and Yoshihiko Kanemitsu[1,a)]
[1]*Institute for Chemical Research and JST-CREST, Kyoto University, Uji, Kyoto 611-0011, Japan*
[2]*Institute for Solid State Physics and JST-CREST, The University of Tokyo, Kashiwa, Chiba 277-8581, Japan*
[3]*Japan Aerospace Exploration Agency, Tsukuba, Ibaraki 305-8505, Japan*

(Received 29 September 2014; accepted 22 December 2014; published online 6 January 2015)

Conventional external quantum-efficiency measurement of solar cells provides charge-collection efficiency for approximate short-circuit conditions. Because this differs from actual operating voltages, the optimization of high-quality tandem solar cells is especially complicated. Here, we propose a contactless method, which allows for the determination of the voltage dependence of charge-collection efficiency for each subcell independently. By investigating the power dependence of photoluminescence decays, charge-separation and recombination-loss time constants are obtained. The upper limit of the charge-collection efficiencies at the operating points is then obtained by applying the uniform field model. This technique may complement electrical characterization of the voltage dependence of charge collection, since subcells are directly accessible.
 [http://dx.doi.org/10.1063/1.4905474]

Shockley and Queisser clarified the influence of unavoidable energy-loss mechanisms on the performance of solar cells.[1] This cleared the way for the development of highly efficient devices, but only an in-depth understanding of the device physics makes maximal efficiencies possible.[2,3] Exceptionally high efficiencies are expected for tandem solar cells, which unify broad absorption and high voltages using series-connected subcells. Such series connections impose a constraint on the conversion efficiency limit (about 50% for three junctions and unconcentrated light). So far, triple-junction solar cells[4] with efficiencies up to 44.4% for concentrated light and 37.9% for unconcentrated light have been realized,[5] and further breakthroughs are expected.

The measurement and comparison of open-circuit voltage and voltage at the operating point are indispensable for optimization.[6–12] The voltage dependent charge-collection (VDCC) efficiency,[13–15] defined as the ratio of carriers collected by the contacts and the photogenerated carriers, is considered to be the most important parameter that determines a solar cell's current–voltage (I–V) performance. The VDCC accounts for the fact that charge-collection efficiency is reduced for operating voltages that are high compared with the short-circuit condition (SCC).

Electrical characterization methods, e.g., I–V and external quantum efficiency (EQE) measurements, have become the prevalent design tools,[9,16] and have been also used for determining the VDCC efficiency of single junctions.[13,14] However, in triple-junction solar cells, either the top or bottom or both sides of a specific subcell cannot be contacted directly. Therefore, EQE measurements require sophisticated light biasing by additional excitation of neighboring subcells at fixed bias (usually SCC).[17] Consequently, it is difficult to accurately verify the VDCC efficiency in a tandem junction only using I–V techniques. Instead, separately grown single junctions have been used as reference to predict the I–V curves of tandem cells.[10] It has been concluded that the junction interfaces of grown tandem cells play a critical role, but are difficult to assess experimentally.[11] To resolve this problem, a contactless method is required for determining the charge-collection efficiency at the operation point of an actual device. Photoluminescence (PL) techniques are promising candidates for its measurement in subcells, since time-resolved PL provides for the evaluation of charge-separation efficiency, while recombination efficiencies for varying carrier densities, corresponding to different voltages, can be examined via power dependence.

In this work, we perform time-resolved PL measurements on an industry-standard triple-junction solar cell, designed for use in space. For both InGaP and GaAs subcells, we observe a systematic change in PL decays when altering excitation-power densities. At low power densities, a fast decay is observed, which is attributed to charge separation under the internal electric field with the carrier mobility. Carrier recombination loss is then determined from spot-size dependence of a dominant slow component, which arises at high power densities. These assignments are confirmed by the numerical calculation of PL decay curves based on the uniform field model. We then evaluate the mobility-limited VDCC efficiencies of both subcells from the experimentally obtained charge-separation and recombination-loss time constants.

The InGaP/GaAs/Ge three-junction solar cell used in this work was characterized by EQE and PL measurements. EQE spectra were measured using a standard technique.[17] For the PL measurements, the sample is not electrically contacted. Time-resolved PL was performed using a mode-locked Ti:sapphire laser for excitation (800 nm, repetition rate: 8 MHz, pulse duration: ≈200 fs) and a Si avalanche

a)Author to whom correspondence should be addressed. Electronic mail: kanemitu@scl.kyoto-u.ac.jp.

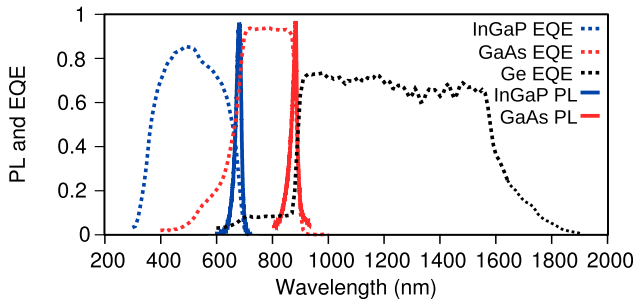

FIG. 1. EQE and PL spectra of subcells in the triple-junction InGaP/GaAs/Ge solar cell designed for use in space.

photo-diode (APD) for detection. Appropriate short and long-pass filters were used to selectively detect the PL of InGaP and GaAs subcells. Second harmonic generation in a beta-barium borate crystal was used to obtain 400 nm. Fast decay components were checked with a tunable laser system (repetition rate 200 kHz) and a streak camera, using filters and a monochromator. The excitation spot sizes, determined by a Si charge-coupled device, were varied between $\approx 15\ \mu$m and 0.65 mm in diameter (full width at half maximum, hereafter $\varnothing$). The PL detection spot was at the center of the excitation spot, extending about $\varnothing 13\ \mu$m. All measurements were performed at room temperature.

Figure 1 shows EQE spectra of the bottom Ge, middle GaAs, and the top InGaP junctions. High EQE values indicate a high-quality device. PL spectra of the subcells are also shown in Fig. 1; the InGaP bandgap energy is 1.8 eV ($\lambda_{InGaP} = 690$ nm), and that of GaAs is 1.42 eV ($\lambda_{GaAs} = 875$ nm). Overlap of EQE spectra is observed for wavelengths with incomplete absorption in a single subcell or photonic coupling between subcells.[18] The PL peak positions are consistent with the EQE cutoff wavelengths.

Figure 2(a) shows the time-resolved PL of InGaP for an excitation spot of $\varnothing 140\ \mu$m at 400 nm with excitation-power densities varied from 0.11 to 7.6 W/cm^2. No additional PL features have been observed for times later than shown. For all powers, GaAs is only weakly excited via spontaneous emission from InGaP, and no laser leakage occurs. As shown in Fig. 2(a), at 0.11 W/cm^2 a single-exponential fast decay with a time constant of 0.25 ns is observed. At intermediate powers, a second decay component appears, which we denote as slow decay. For elevated powers, the slow decay becomes longer and more pronounced. At 7.6 W/cm^2, two single-exponential decays are observed. The saturated slow decay has a time constant of 7 ns. Other decay features are the initial ultrafast decay ($t < 0.2$ ns, due to surface recombination, but not resolved) and the small tail towards the end of the decays (this may be, for example, PL due to a diffusion limited recombination process), but these are not discussed in this letter.

In Fig. 2(b), the PL behavior is analyzed with respect to the power dependence of the slow and fast time constants. The decay was measured at time $t = 0.9$ ns, which suppresses the influence of initial-measurement artifacts due to instrument response time. At low excitation-power densities (<1.2 W/cm^2), a constant fast decay is observed. This constant region defines τ_1. Measurements with a streak camera revealed that $\tau_1 = 0.08$ ns is faster than the resolution of the APD system (about 0.25 ns). At higher power densities, a slower decay is observed; at 6 W/cm^2, the slow component saturates, defining τ_2. Since τ_2 was same for repetition rates 8 MHz and 800 kHz, the effect of long-lived carriers is considered to be small.

Figure 2(c) shows that τ_2 depends on the excitation spot size. The solid and dotted lines are a guide to the eye (a basic linear function), indicating that τ_2 becomes longer for larger spot diameter d, which is attributed to lifetime-enhancing effects such as photon recycling. By decreasing the spot size, the excitation volume decreases drastically, and thus effects from photon recycling are suppressed. For InGaP, we estimate the intrinsic time constant $\tau_2(d = 0) = \tau_{loss} = 2$ ns.

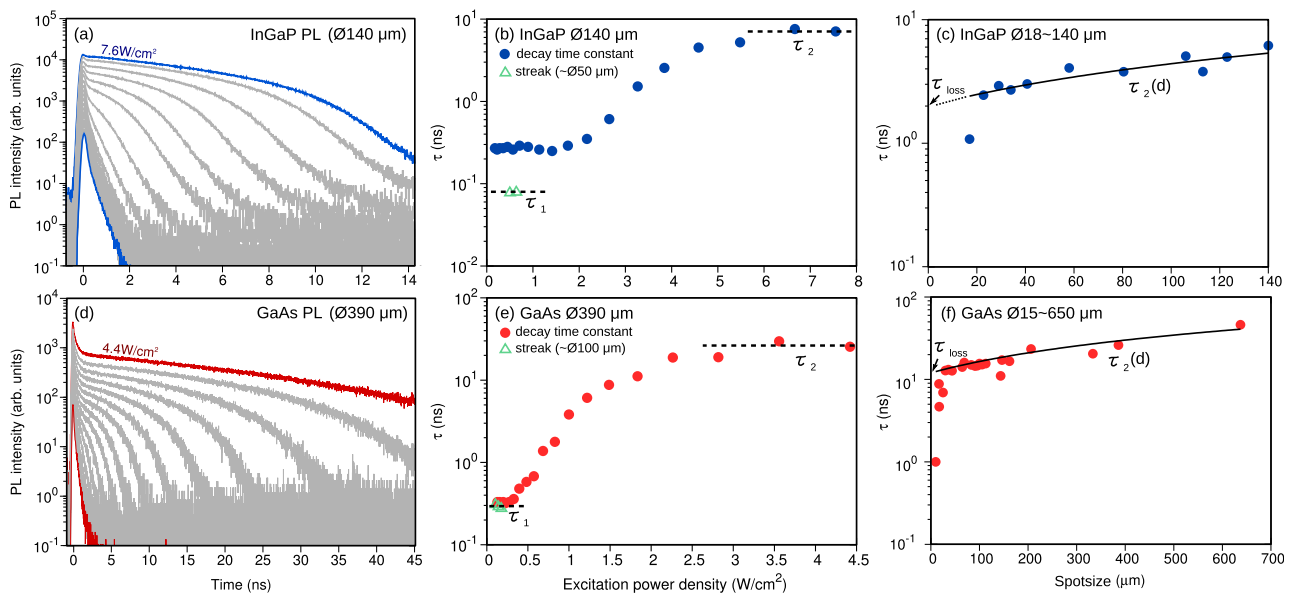

FIG. 2. (a) Time-resolved PL for InGaP. Spot size: $\varnothing 140\ \mu$m. Excitation: 400 nm, power densities ranged from 0.11 to 7.6 W/cm^2. (b) Power dependence of slow and fast components of InGaP. Spot size: $\varnothing 140\ \mu$m. Green triangles: streak-camera measurements. Dotted lines indicate constant values of τ. (c) Spot-size dependence of saturated time constant τ_2 in the InGaP subcell. Black lines are guides-to-the-eye using a linear function. (d) Time-resolved PL for GaAs. Spot size: $\varnothing 390\ \mu$m. Excitation: 800 nm, power densities changed from 0.09 to 4.4 W/cm^2. (e) Power dependence for slow and fast components of GaAs. Spot size: $\varnothing 390\ \mu$m. (f) Spot-size dependence for the saturated time constant τ_2 in the GaAs subcell.

Similar dynamic behaviors are also observed in the GaAs subcell. The time-resolved PL obtained for the excitation of GaAs at 800 nm is shown in Fig. 2(d). Here, the excitation spot size was ∅390 μm, while power density was varied between 0.09 and 4.4 W/cm^2. A fast decay is observed at low excitation-power densities and a slow decay component appears at high excitation-power densities. The initial PL peak ($t < 2$ ns) found at higher power densities is assigned to PL from the entire junction, before fast carrier re-distribution settled down.

Figure 2(e) shows the power dependence of slow and fast decay-time constants. For power densities up to 0.5 W/cm^2, the decay was measured at about 2 ns. Above 0.5 W/cm^2, the slow decay was measured at 4.0 ns to suppress influence from the initial PL from the entire junction. The constant value at low power (<0.3 W/cm^2) defines $\tau_1 = 0.29$ ns, and the saturated (>3 W/cm^2) value of the slow component defines τ_2.

The excitation spot-size dependence for GaAs is shown in Fig. 2(f). Below 30 μm, the slow time constant abruptly shortens, which is attributed to dominant in-plane bulk diffusion. This region is excluded when determining $\tau_2(d=0) = \tau_{loss} = 12$ ns. Note that the time constants for the GaAs subcell are much larger than those of the InGaP subcell.

With regard to the mechanisms governing the PL decays, we consider that PL from the active region (AR), usually centered around the intrinsic layer or depletion region, dominates the PL dynamics in our samples. Carriers in the AR can recombine, but can also be swept out by the internal electric field (=charge collection). Figure 3(a) shows a subcell band diagram for low and high excitation-power densities. For low densities, the number of carriers in the junction is too small to increase the voltage, i.e., diffusion current is small. In this case, the carriers are swept out from the AR, which quickly diminishes PL. The sweep-out time depends on the internal electric field and the carrier mobility. At high densities, the junction approaches a flat-band condition. This enhances band-to-band recombination, and the loss mechanisms will limit the PL decay, resulting in slow decay.

We consider that τ_2 is proportional to recombination losses in the sample, and τ_1 is determined mainly by charge separation, constituting the charge-collection time constant. This assignment is consistent with the numerical calculation based on the equation given below.

The rate equation for the PL intensity I_{PL} in the AR can be simplified as

$$\frac{dI_{PL}}{dt} = -\frac{I_{PL}}{\tau_{loss}} - \frac{I_{PL}}{\tau_1}\left(1 - \frac{V(I_{PL})}{V_g}\right), \quad (1)$$

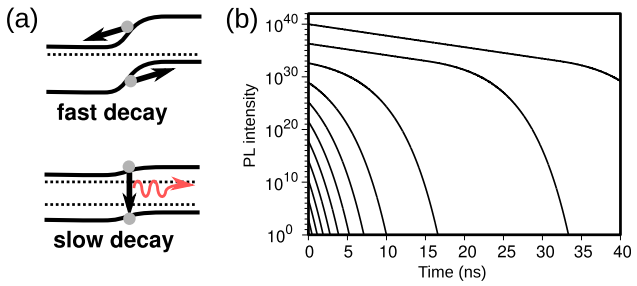

FIG. 3. (a) Subcell band diagram for low and high excitation powers. (b) Theoretical calculation of PL decay curves at different excitation powers.

with an intensity-dependent junction voltage $V(I_{PL})$. Recombination losses are expressed by the first term on the right side of Eq. (1); the charge separation is expressed by the second.

The voltage dependence in Eq. (1) is the analytic shape predicted by the uniform field approximation[15] in the low-field limit (close to the operating point) and the linear field dependence of the drift time (e.g., Eqs. (6)–(9), Ref. 14). Although the actual field in the junction is not necessary uniform, the uniform field approximation can be quite reasonable, as long as carrier densities are not too high.[14,19] For zero voltage, the charge collection becomes dominant, since $\tau_1 \ll \tau_{loss}$. The upper limit for the voltage is the gap voltage V_g (a limit of the built-in voltage). This limit occurs because τ_1 is mainly determined by the built-in electric field, as confirmed by the power dependence in Figs. 2(b) and 2(e). If diffusion of photogenerated carriers from the p and n regions becomes important, which occurs under higher illumination powers, the effective drift velocity will be reduced and a smaller voltage has to be used for normalization, i.e., only when both drift and diffusion are considered, the use of V_{oc} is possible. At $V = V_g$, the last term becomes zero and τ_{loss} dominates the slow PL decay.

The analytical shape of $V(I_{PL})$ depends on the sample, but may be approximated with that obtained from the Boltzmann relations[20]

$$I_{PL} \propto \exp\frac{qV(I_{PL})}{k_B T}, \quad (2)$$

where q is the elementary charge, k_B is the Boltzmann constant, and T is the sample temperature. The physics embodied by this idealized equation is simple, yet serves as a good test to elucidate our interpretation of τ_1 and τ_{loss}. Several solutions for Eq. (1) are shown in Fig. 3(b). Here, we used parameters near to the experimental values for InGaP ($\tau_1 = 0.08$ ns, $\tau_{loss} = 2$ ns, $V_g = 1.8$ V). For low intensities, a fast decay is observed, while a slow decay becomes dominant for high intensities. The main features of the experimental PL decays can be directly explained by the uniform field model, and thus we believe it is valid.

Here, we used the simplified rate equation (Eq. (1), which neglects diffusion) for a clear understanding of the physical processes determining charge collection. A detailed system of rate equations, accounting for the different regions of the junction, is important for a rigorous test. While τ_2 is an indicator of the losses in the AR, the fast decay observed at high excitation power is strongly influenced by losses in the p and n regions and also diffusion from there. The additional analysis of this decay enables more accurate description of the solar cell under steady-state condition.[21]

Using the uniform field approximation, the charge-collection efficiency of each subcell, which is a function of the subcell operating voltage V, is given by

$$\eta_c(V) = \frac{1}{1 + \frac{\tau_1}{\tau_{loss}}\frac{1}{1 - \frac{V}{V_g}}}, \quad (3)$$

directly derived from Eq. (1). Since we defined η_c with τ_1, back-diffusion losses[19] are not included. Consequently, a

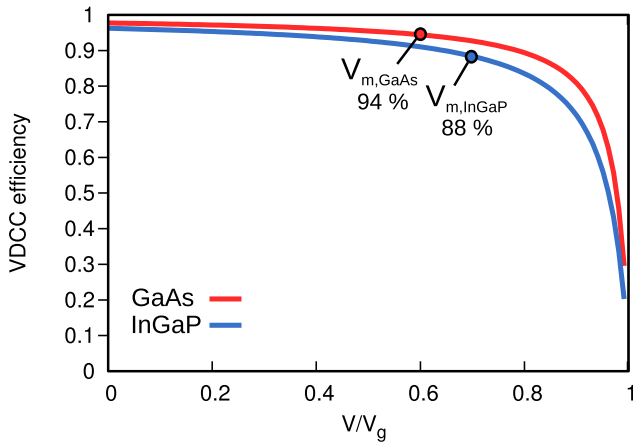

FIG. 4. VDCC efficiencies for $\eta_c(V)$ of InGaP ($\tau_1 = 0.08$ ns, $\tau_{loss} = 2$ ns) and GaAs ($\tau_1 = 0.29$ ns, $\tau_{loss} = 12$ ns) subcells. The values for the point of maximum power ($V_m \approx 0.6$ and $0.7V_g$ for GaAs and InGaP, respectively) are shown as open black circles.

well defined upper limit of the charge-collection efficiency is obtained, useful for subcell analysis. As mentioned above, the definition with τ_1 also requires V_g to be used. The voltage dependence of $\eta_c(V)$ for both subcells is shown in Fig. 4. The VDCC of GaAs (Fig. 4, red line) has a very high and flat efficiency for low voltages ($V/V_g < 0.8$) and quickly drops to zero for higher voltages. As with the I–V curves, the fill factor (FF) of the GaAs VDCC curve is large, indicating high carrier mobility. The VDCC of InGaP (Fig. 4, blue line) shows a reduced overall efficiency and a smoother drop to zero, indicating stronger dependence on nonradiative recombinations. As such, this curve evidences that the material quality of InGaP is still an issue for solar cell devices.[22]

It is noted that the EQE values shown in Fig. 1 are usually obtained for the SCC of the subcell. Transport losses are always included in EQE measurements, but their influences are suppressed in optical measurements. Therefore, the differences between EQE and $\eta_c(V)$ curves are helpful for the analysis of transport losses, i.e., series resistances.

Additionally, we stress that for achieving maximal efficiencies, the differences due to *voltage changes at the operating point* can be crucial for current matching. In subcells with low FF, the VDCC efficiency itself changes significantly, even for small voltage changes (for example, the InGaP curve in Fig. 4 has a comparable steep drop near the point of maximum power V_m). Thus, the evaluated VDCC curve represents a more accurate description of the device than the constant EQE value. In other words, the accuracy of the VDCC efficiency is derived from voltage-dependent behavior close to that of the real device, rather than from a highly accurate lifetime determination.

By measuring PL decays, the two essential parameters τ_1 and τ_{loss} are obtained. The mobility-limited charge-collection efficiencies near the actual operating voltages are calculated, and can be used to analyze I–V behavior. We found significantly smaller values at the operating point than at SCC, which accounts for additional voltage drops at the operating point, and thus explains losses in subcells that have not been predicted by conventional electrical evaluation.

In summary, we measured PL decay curves as a function of excitation intensity from the top and middle junctions of a triple-junction solar cell designed for use in space. Since the carrier-density dependence of the PL decay corresponds to the voltage dependence of carrier separation and recombinations, we evaluated the voltage dependence of the charge-collection efficiency for as-grown subcells, including their interfaces. An experimentally obtained carrier-extraction behavior should enable more accurate device simulations and improvements compared to other methods relying on reference cells or light biasing.

Part of this work was supported by JST-CREST and the Sumitomo Electric Industries Group CSR Foundation.

[1]W. Shockley and H. J. Queisser, J. Appl. Phys. **32**, 510 (1961).
[2]O. D. Miller, E. Yablonovitch, and S. R. Kurtz, IEEE J. Photovoltaics **2**, 303 (2012).
[3]L. Zhu, C. Kim, M. Yoshita, S. Chen, S. Sato, T. Mochizuki, H. Akiyama, and Y. Kanemitsu, Appl. Phys. Lett. **104**, 031118 (2014).
[4]T. Takamoto, M. Kaneiwa, M. Imaizumi, and M. Yamaguchi, Prog. Photovoltaics: Res. Appl. **13**, 495 (2005).
[5]See http://www.nrel.gov/ncpv/images/efficiency_chart.jpg for a summary of the world-record solar-cell efficiencies.
[6]A. D. Vos, J. Phys. D: Appl. Phys. **13**, 839 (1980).
[7]C. H. Henry, J. Appl. Phys. **51**, 4494 (1980).
[8]P. Baruch, A. De Vos, P. T. Landsberg, and J. E. Parrott, Sol. Energy Mater. Sol. Cells **36**, 201 (1995).
[9]R. Hoheisel, F. Dimroth, A. W. Bett, S. R. Messenger, P. P. Jenkins, and R. J. Walters, Sol. Energy Mater. Sol. Cells **108**, 235 (2013).
[10]Q. H. Fan, X. Liao, X. Xiang, C. Chen, G. Hou, X. Cao, and X. Deng, J. Phys. D: Appl. Phys. **43**, 145101 (2010).
[11]B. Bills, X. Liao, D. W. Galipeau, and Q. H. Fan, IEEE Trans. Electron Devices **59**, 2327 (2012).
[12]S. Chen, L. Zhu, M. Yoshita, T. Mochizuki, C. Kim, H. Akiyama, M. Imaizumi, and Y. Kanemitsu, Thorough subcells diagnosis in a multi-junction solar cell via absolute electroluminescence-efficiency measurements, Sci. Rep. (in press).
[13]S. Hegedus, Prog. Photovoltaics: Res. Appl. **5**, 151 (1997).
[14]S. Hegedus, D. Desai, and C. Thompson, Prog. Photovoltaics: Res. Appl. **15**, 587 (2007).
[15]R. S. Crandall, J. Appl. Phys. **54**, 7176 (1983).
[16]M. Meusel, C. Baur, G. Letay, A. W. Bett, W. Warta, and E. Fernandez, Prog. Photovoltaics: Res. Appl. **11**, 499 (2003).
[17]J. Burdick and T. Glatfelter, Solar Cells **18**, 301 (1986).
[18]S. H. Lim, J.-J. Li, E. H. Steenbergen, and Y.-H. Zhang, Prog. Photovoltaics: Res. Appl. **21**, 344 (2013).
[19]K. Misiakos and F. A. Lindholm, J. Appl. Phys. **64**, 383 (1988).
[20]S. M. Sze, *Physics of Semiconductors Devices*, 2nd ed. (Wiley, New York, 1981).
[21]D. M. Tex, T. Ihara, H. Akiyama, M. Imaizumi, and Y. Kanemitsu (unpublished).
[22]J. F. Geisz, M. A. Steiner, I. Garcia, S. R. Kurtz, and D. J. Friedman, Appl. Phys. Lett. **103**, 041118 (2013).